A novel G protein-coupled receptor, related to GPR4, is required for assembly of the cortical actin skeleton in early *Xenopus* embryos

Qinghua Tao[1], Brett Lloyd[1,2], Stephanie Lang[1], Douglas Houston[1,*], Aaron Zorn[1] and Chris Wylie[1,†]

[1]Division of Developmental Biology, Cincinnati Children's Research Foundation, 3333 Burnet Avenue, Cincinnati, OH 45229, USA
[2]Physician Scientist Training Program, University of Cincinnati College of Medicine, University of Cincinnati College of Medicine, PO Box 670555, Cincinnati, OH 45267, USA
*Present address: University of Iowa, Department of Biology, Iowa City, IA 52242, USA
†Author for correspondence (e-mail: christopher.wylie@cchmc.org)

Accepted 18 April 2005

Development 132, 2825-2836
Published by The Company of Biologists 2005
doi:10.1242/dev.01866

Summary

As the fertilized *Xenopus* egg undergoes sequential cell divisions to form a blastula, each cell develops a network of cortical actin that provides shape and skeletal support for the whole embryo. Disruption of this network causes loss of shape and rigidity of the embryo, and disrupts gastrulation movements. We previously showed that lysophosphatidic acid (LPA) signaling controls the change in cortical actin density that occurs at different stages of the cell cycle. Here, we use a gain-of-function screen, using an egg cDNA expression library, to identify an orphan G protein-coupled cell-surface receptor (XFlop) that controls the overall amount of cortical F-actin. Overexpression of XFlop increases the amount of cortical actin, as well as embryo rigidity and wound healing, whereas depletion of maternal *XFlop* mRNA does the reverse. Both overexpression and depletion of XFlop perturb gastrulation movements. Reciprocal rescue experiments, and comparison of the effects of their depletion in early embryos, show that the XLPA and XFlop signaling pathways play independent roles in cortical actin assembly, and thus that multiple signaling pathways control the actin skeleton in the blastula.

Key words: Cortical actin, G protein coupled receptor, *Xenopus*

Introduction

The actin skeleton controls many aspects of cell behavior (reviewed by Revenu et al., 2004). However, little is known of how cortical actin is assembled in early embryos, or how it is remodeled as cell behavior changes during morphogenesis. The early *Xenopus* embryo is a useful system in which to analyze this process. The expression of individual cytoskeletal elements can be either up or downregulated during early development by mRNA injection or antisense oligodeoxynucleotide-mediated mRNA depletion, respectively, and the consequences to the cytoskeletal pattern and to normal development assayed in an in vivo system (Quaas and Wylie, 2002; Robb et al., 1996; Torpey et al., 1992; Vernos et al., 1995).

We have previously shown that the *Arm* repeat protein Plakoglobin (γ catenin) is both necessary and sufficient for assembly of the cortical actin skeleton in early *Xenopus* embryos, and is downstream of the signaling intermediate cdc42 (Kofron et al., 2002). In order to identify more fully the pathways leading to cortical actin assembly, an arrayed two- to four-cell cDNA library was divided into mRNA pools, which were expressed in *Xenopus* embryos by microinjection at the two-cell stage. Pools that caused effects similar to plakoglobin/cdc42 overexpression were split in a matrix fashion (Grammer et al., 2000) to identify the active mRNAs. One of these mRNAs was found to encode a novel G protein-coupled receptor (GPCR), whose sequence is related to a subfamily of GPCRs, the OGR1 (Ovarian cancer G protein-coupled Receptor 1) subfamily. Overexpression of this mRNA dramatically increased the density of the actin skeleton in the early *Xenopus* embryo, whereas oligodeoxynucleotide-mediated depletion of the endogenous mRNA had the reverse effect, and caused embryos to lose their shape and rigidity. On the basis of the phenotype caused by its depletion, we have given this protein the provisional name of XFlop. In a previous paper, we showed that intercellular signaling is required to maintain the normal density of the cortical actin skeleton in *Xenopus*, and that the expression of LPA receptors is both necessary and sufficient to maintain the normal density of cortical actin filaments in interphase cells (Lloyd et al., 2005). Here, we compare the roles of these two ligand receptors, and conclude that they each play independent roles in generating the normal pattern of actin filaments in the embryo. Thus, multiple cell signaling pathways are involved in this process.

Materials and methods

Gain-of-function library screen

Approximately 16,000 colonies from a *Xenopus* two- to four-cell cDNA expression library were arrayed into 38 384-well plates using a QBot (Genetix). Each master plate was split into four 96-well plates (denoted as nA, nB, nC, nD, where n=1-38). After 2-3 days incubation, colonies from each 96-well plate were pooled for plasmid isolation and capped RNA synthesis. 5 ng mRNA from each pool was injected into the animal cytoplasm of two-cell-stage *Xenopus* eggs. Injected embryos were reared in 0.2×MMR containing 2% Ficoll, and were analysed for cortical actin assembly at the late blastula stage (Stage 9) (Nieuwkoop, 1975). To identify the active colonies from the first-round mRNA pools,

active pools from the master plates were amplified in triplicate in 96-well plates (one for the 2nd round screen, one for the 3rd round screen, one for backup). In the 2nd round screen, the eight wells from each column of a 96-well plate were pooled, and 1-2 ng of mRNA from each column was analysed as before. In the 3rd round screen, mRNAs were transcribed from the eight single wells from the active column. Finally, if a mRNA from a single colony mimicked the effect of the original pool, it was sequenced for further analysis. All 384-well and 96-well plates were from Genetix. Each well was filled with 200 μl LB medium containing 8% glycerol, and plates were kept in a humidified chamber to minimize evaporation. The alkali lysis protocol was used for all library plasmid isolation. The plasmids were linearized with *Not*I and transcribed with SP6 Message Machine kit (Ambion).

Cortical actin-assembly assays and pixel-intensity analysis

Cortical actin assembly assays were carried out exactly as described previously (Kofron et al., 2002; Lloyd et al., 2005). The size of each confocal image was set as 512×512 pixels. Z stacks, that include cortical actin of all the superficial cells of the blastocoelic surface of the cap, are shown in all low power (20×) pictures of entire caps. The intensity of each pixel was calculated by Zeiss 510 software in a linear range of 128-4095 (2-256 for the older version of software). The overall amount of the cortical actin for each cap is expressed as mean pixel intensity across the whole cap. Five to eight caps from each treatment were analyzed in all experiments, and the results presented as mean pixel intensity ±s.d. Treatments were compared for statistical significance by Student's *t*-test.

mRNA depletion and host transfers

These were carried out as described previously (Kofron et al., 2002). Briefly, stage VI oocytes were obtained by manual defolliculation and cultured in oocyte culture medium (OCM). To deplete the maternal store of XFlop mRNA, 8-12 ng of HPLC-purified antisense phosphorothioate-modified oligodeoxynucleotides (18-mer) were injected into each oocyte. After 2-3 days of culture at 18°C, oocytes were matured and transferred using host transfer techniques (Holwill, 1987). The sequences of two antisense oligonucleotides used to deplete maternal *XFlop* mRNA are: oligo 1s, 5′-A*A*-G*GGAACACTGTAG*C*C*A-3′; oligo 5s, 5′-G*T*T*GT-ACGTTTTGGC*T*G*G-3′, where * indicates the phosphorothioate diester bond substitution.

mRNA synthesis and injection

Plasmids from the expression library, and those encoding pCS2$^+$ XFlop ΔC and FL were linearized with *Not*I and transcribed in vitro using SP6. *XFlop* mRNA (10-250 pg) was injected into the animal cytoplasm at the two- or eight-cell stage. mRNA-injected embryos were reared in 0.2×MMR containing 2% Ficoll, and transferred to 0.1×MMR at the mid-blastula stage.

Total RNA isolation and real-time RT-PCR

These were performed exactly as described previously (Kofron et al., 2002).

Immunostaining

Microtubules and cytokeratin filaments in control and XFlop-depleted animal caps were detected as described previously (Kofron et al., 2002).

Results

Gain-of-function screen for maternal genes involved in actin assembly

We constructed a *Xenopus* two- to four-cell-stage cDNA expression library, using oligo dT-primed polyA$^+$ RNA directionally cloned into the *Xenopus* expression plasmid pCS2$^+$. The library contains 1×10^6 independent clones, with an average insert size of >1 kb. The library was plated, and mRNA pools generated, as decribed in the Materials and methods. mRNA pools were injected in 5 ng doses (representing 50 pg of each mRNA) into the animal cytoplasm of two-cell-stage embryos. The embryos were allowed to develop to the late blastula stage (Fig. 1A). Animal caps (Fig.

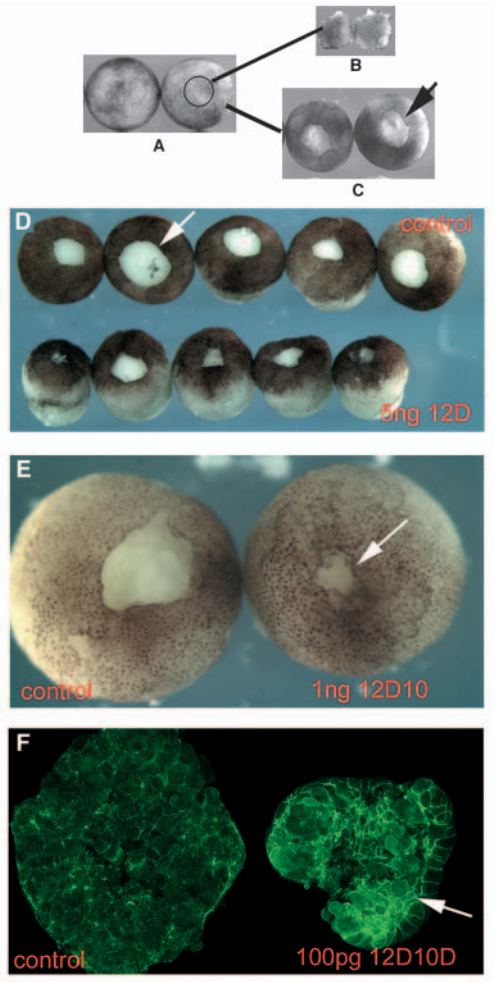

Fig. 1. (A-C) Plan of the assays used in this study. Animal caps (B) were excised from embryos at the late blastula stage (A) and cultured for 10 minutes before fixation and staining for F-actin. The remainder of the embryos, the bases (C), were cultured for 1-2 hours to assay the degree of rigidity, the shape, and the ability to heal the wound left by animal cap excision. (D) Embryos from which the animal caps were removed 45 minutes previously: control embryos (upper row) and embryos injected at the two-cell stage with 5 ng mRNA from pool 12D (lower row). 12D-expressing embryos are more compact and rigid, and have an exaggerated wound-healing response. The margin of one of the wounds is indicated (arrow, D). (E) A control embryo (left), and an embryo injected with 1 ng mRNA from pool 12D, column 10 (right), treated identically to those embryos shown in D. The more rapidly healing wound of the 12D10-injected embryo is indicated (arrow). (F) Alexa-488 conjugated Phalloidin staining of animal caps from a control embryo (left) and an embryo injected with 100 pg mRNA from the single pool 12D10D (right). The animal cap expresses increased levels of cortical actin and has an exaggerated wound response. The purse-string that forms the boundary between the inside and outside surfaces of the cap is indicated in the 12D10D-injected cap (arrow). mRNA from this clone mimicked all of the effects of the whole pool 12D, and the column 12D10.

1B) were excised and cultured until the debris from dead cells could be removed (10 minutes). Caps were then fixed, Alexa-488 phalloidin stained, and examined under the confocal microscope for the presence, pattern and density of cortical actin staining. The remainder of the embryos after excision of the caps, the bases (Fig. 1C), were assayed for rigidity, shape, and the ability to heal the wound left by the excision of the animal cap. Pooled mRNAs from eight of the 96-well plates caused dramatic changes in the actin skeleton. Colonies were pooled from each column of wells from positive 96-well plates. mRNA was transcribed from these, and injected in doses of 1 or 2 ng (representing 125 pg and 250 pg, respectively, of each mRNA) into embryos at the two-cell stage, and assayed as before. Finally, mRNA was transcribed from each well of the positive columns, and doses of 100 pg and 200 pg assayed to identify the active maternal cDNA.

In this paper, we report on the role in actin assembly of one clone identified in this screen, 12D10D, which encodes a novel G protein-coupled receptor. Fig. 1D shows that embryos injected with mRNA from pool 12D were more rigid and spherical than controls; the wound made by excision of the animal cap is arrowed. Fig. 1E shows the dramatic enhancement in wound healing, 45 minutes after animal cap removal, in embryos injected with mRNA from the single column 12D10 of colonies. Fig. 1F shows that animal caps dissected from late blastulae injected at the two-cell stage with 100 pg of mRNA from the single colony 12D10D healed faster than control caps, and contain dramatically increased cortical actin. The same results were seen in embryos injected with the original pool, the active column, and the single active colony. In each case, batches of 5-10 embryos were examined, and five to six caps were analyzed. In each case the results were identical to the representative samples shown in Fig. 1D-F.

Based upon the effect of its depletion in the early embryo (see below), we temporarily named this protein XFlop, until a more systematic name, based upon function and structure, can be allocated.

Characterization and expression pattern of XFlop

Three independent colonies from 12D10D were sequenced in both strands. The sequence has been deposited in GenBank (AY766161). The *XFlop* cDNA sequence is 1.5 kb long. The predicted open reading frame encodes a protein of 348 amino acids (Fig. 2A), which contains a seven-pass transmembrane domain, suggesting that XFlop is a G protein-coupled receptor (GPCR). Furthermore, XFlop contains a putative N-linked glycosylation site (N*QSC, aa4-7) in the N-terminal extracellular domain (aa1-aa18), and a conserved acidic-arginine-aromatic triplet (D-R-F) in the N-terminal extremity of the second cytoplasmic loop (aa111-aa113), each characteristic of GPCRs (Bause, 1983; Wheatley and Hawtin, 1999). The acidic-R-aromatic triplet has been implicated in G-protein coupling (Oliveira et al., 1994). XFlop shows 46-53% sequence homology with members of a recently proposed subfamily including mammalian ovarian cancer G protein-coupled receptor 1 (OGR1), G protein-coupled receptor 4 (GPR4), G2 accumulation (G2A) and T cell death-associated gene 8 (TDAG8) (Fig. 2B) (Heiber et al., 1995; Xu, 2002).

Recently, another member of the GPR4 family was identified in *Xenopus* (Xgpcr4) (Chung et al., 2004). Fig. 2A shows that the putative amino acid sequences are very divergent in the C termini of Xgpcr4 and XFlop, which suggests that they are encoded by different genes that are not pseudoalleles of the same gene. We also found that Xgpcr4 and XFlop are encoded by different genomic sequences even though they reside in the same chromosome (Fig. 2C). Comparison with the genomic scaffold sequence (Scaffold 3407, JGI) shows that the ORF of XFlop is encoded by a single exon, a feature shared by mammalian GPR4 proteins (Heiber et al., 1995).

Comparison of the sequence of the original 12D10D clone with the contig sequence from the NIBB database suggested that there might be a single adenosine insertion at position 947 in the open reading frame of the 12D10D clone (Fig. 2D, highlighted in green), which would result in a premature translation stop, affecting the C-terminal 30 amino acids (Fig. 2A). To establish which coding sequence is expressed in the embryo, we used the contig-coding sequence to PCR-amplify the putative full-length coding sequence from a late blastula cDNA preparation. Sequencing of the amplified cDNA showed that the original 12D10D clone did indeed contain a single adenosine insertion at nucleotide 947. We further compared this cDNA sequence with the *Xenopus tropicalis* genomic sequence (scaffold 3407) available from the JGI database, which further supported the notion that the adenosine insertion in the 12D10D clone is an artifact of library construction. Fig. 2D compares the coding sequences of the 12D10D clone and the full-length cDNA isolated from late blastula mRNA, and shows that the 12D10D clone has a stop codon earlier than in the full-length sequence. We therefore denoted the original 12D10D sequence as *XFlop ΔC*. Interestingly, these two forms of the protein had exactly the same activities in regulating actin assembly (see below), suggesting that the C-terminal 30 amino acids are not required for the action of XFlop on the actin skeleton.

To assay the spatial and temporal expression pattern of *XFlop* mRNA during early development, we made cDNA from embryos frozen at different stages, and assayed the level of *XFlop* mRNA by quantitative real-time PCR. XFlop was expressed maternally, and ubiquitous expression was observed in the blastula throughout early development (Fig. 2E).

Overexpression of XFlop accelerated wound healing and enhanced actin assembly

We transcribed both *XFlop ΔC* and full-length *XFlop* mRNA and microinjected them, in doses of between 10 and 250 pg per embryo, into the animal cytoplasm at the two-cell stage. After excision of animal caps at the late blastula stage, the remainder of the embryos (the bases) were found to heal significantly faster than controls (Fig. 3A,E, compare blue and yellow bars), in a dose-dependent fashion. The blastocoel roofs of *XFlop*-injected embryos were also thicker than those of controls (Fig. 3B). The mean (±s.d.) thickness of the blastocoel roofs (the distance from the middle of the roof to the animal pole) was measured in ten embryos from photographs of fixed, bisected embryos. The mean roof thickness (±s.d.) of XFlop-overexpressing embryos was 195±37 μm, which compared with 73±25 μm for control embryos.

The effect of XFlop overexpression on cortical actin is shown in Fig. 3C,D. At low magnification, the level of staining in the whole cap is dramatically increased, as shown by the pixel intensity charts (Fig. 3C). The mean pixel intensity of five to eight caps (±s.d.) is shown in Fig. 3D, together with the *P*-

value from the comparison by Student's *t*-test of the control, and mean and standard deviation of a 250 pg dose. Increasing doses of *XFlop* mRNA caused a corresponding increase of phalloidin binding, and therefore of F-actin concentration in the cell cortices. Examination of individual caps showed that not all cells have increased actin staining (arrow in Fig. 3C).

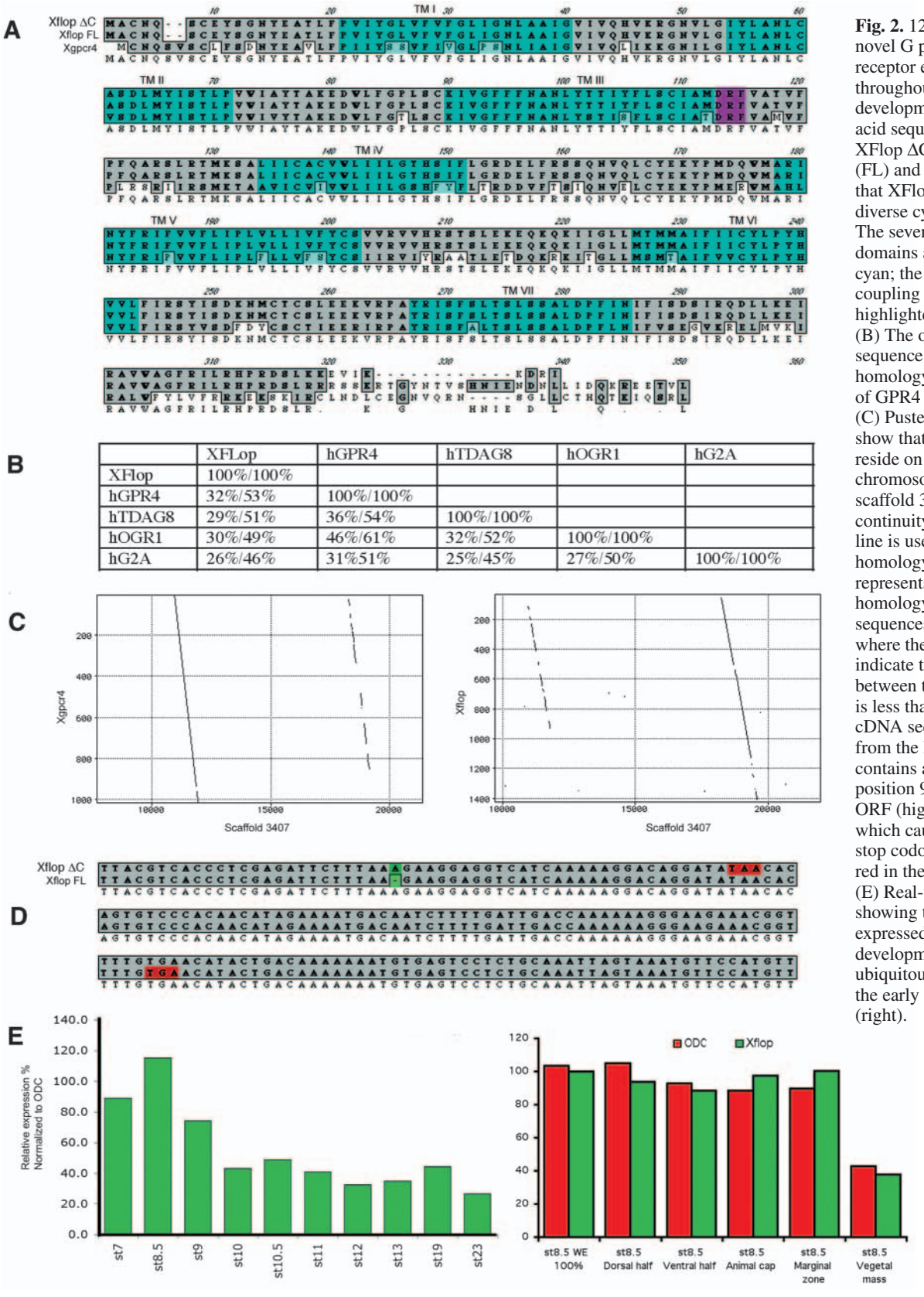

	XFLop	hGPR4	hTDAG8	hOGR1	hG2A
XFlop	100%/100%				
hGPR4	32%/53%	100%/100%			
hTDAG8	29%/51%	36%/54%	100%/100%		
hOGR1	30%/49%	46%/61%	32%/52%	100%/100%	
hG2A	26%/46%	31%51%	25%/45%	27%/50%	100%/100%

Fig. 2. 12D10D encodes a novel G protein-coupled receptor expressed throughout early *Xenopus* development. (A) Amino acid sequence alignment of XFlop ΔC, full-length XFlop (FL) and Xgpcr4, showing that XFlop and Xgpcr4 have diverse cytoplasmic tails. The seven transmembrane domains are highlighted in cyan; the putative G protein-coupling motif (DRF) is highlighted in mauve. (B) The overall percentage sequence identity and homology among members of GPR4 subfamily. (C) Pustell matrix analyses show that XFlop and Xgpcr4 reside on the same chromosome (represented by scaffold 3407). The continuity of the plotting line is used to represent homology: a solid line represents greater than 65% homology between the two sequences, whereas areas where the line is broken indicate that the homology between the two sequences is less than 65%. (D) The cDNA sequence identified from the library screen contains an extra A at position 947 of the putative ORF (highlighted in green), which causes a premature stop codon (highlighted with red in the upper row). (E) Real-time RT-PCR data showing that XFlop is expressed throughout early development (left), and is ubiquitously expressed in the early to late blastulae (right).

This could be due to one of two possibilities. First, the injected mRNA may not have filled this area of the injected embryo. This is unlikely, as cells surrounding the injected one have increased actin staining. Second, and more likely, we have shown previously that cells undergoing cytokinesis change their cortical actin to a less-dense network (Lloyd et al., 2005). As cells divide normally in XFlop-overexpressing embryos, it is likely that they go through the same cycles of actin assembly and disassembly during the cell cycle. However, we have not experimentally discriminated between these two possibilities.

Higher magnification images of control and XFlop-overexpressing animal caps are shown in Fig. 4. Cortical actin is increased in both inner (Fig. 4A,B) and outer (Fig. 4C,D) surfaces of the caps. Interestingly, all actin-containing structures show an increased intensity of staining. The cortical network is denser, regions where cells overlap show increased staining, and there is an increased density of small projections from the cell surfaces. The fact that no actin-containing structures are enhanced at the expense of others, and that there is not any change in the type of network or processes, suggests that XFlop may control the overall amount of F-actin polymerization, rather than controlling any specific actin-containing structure in the embryonic cells.

XFlop and XLPA receptor overexpression both cause increased cortical actin assembly. We sought to exclude the possibility that this is a general property of G protein-coupled receptor-mediated signaling by testing the effects of overexpression of two other G protein-coupled receptors: TDAG8 (which is in the same sub-family in mammals) and the distantly related GPR160. In each case, 200 pg of full-length mRNA was injected into two-cell-stage embryos, and the animal caps assayed as above at the late blastula stage. In both

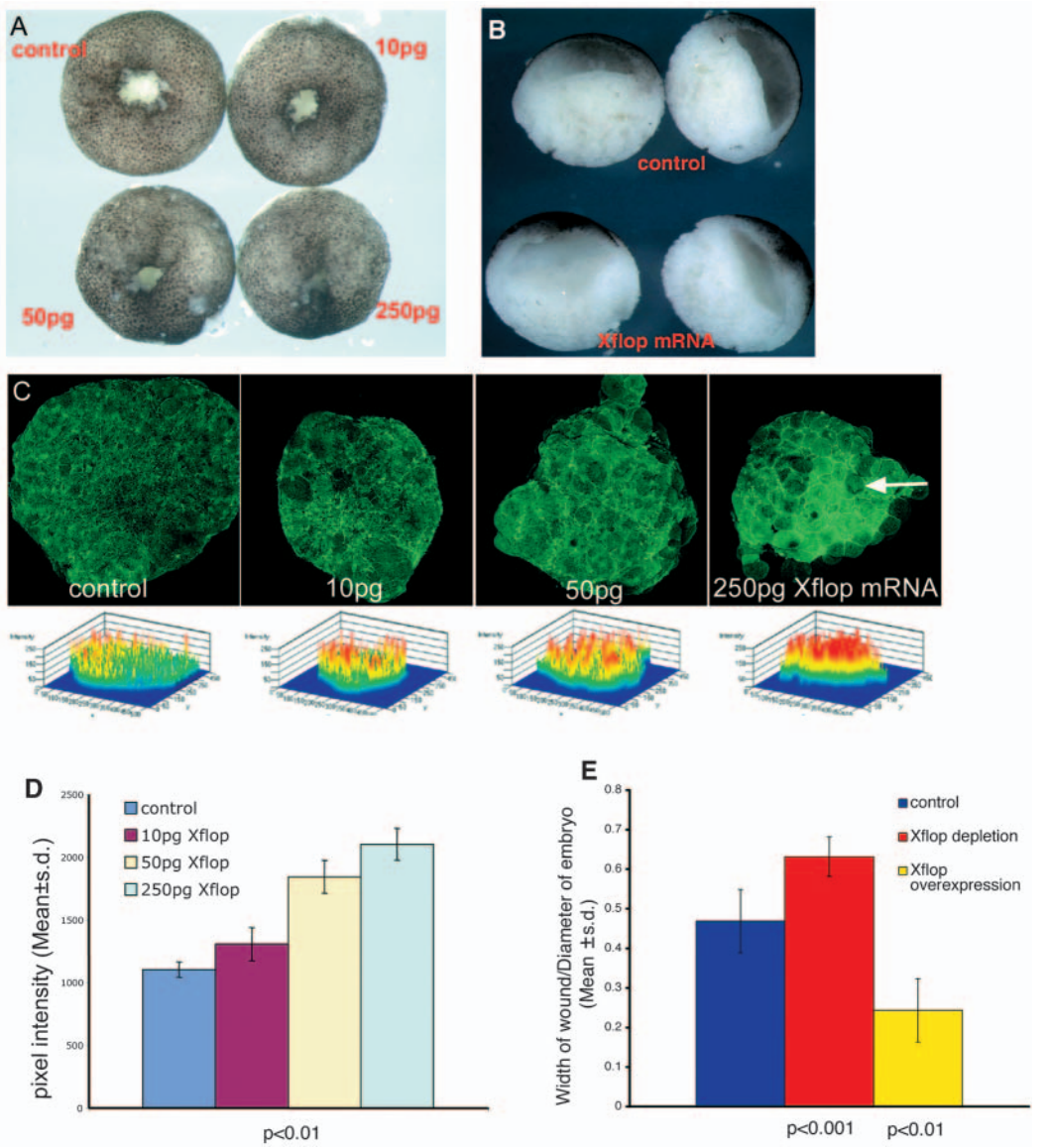

Fig. 3. XFlop is sufficient for actin assembly in early *Xenopus* embryos. (A) XFlop increases the rate of the wound healing in a dose-dependent manner. Photographs were taken 45 minutes after the excision of animal caps from embryos injected at the two-cell stage with 10-250 pg doses of *XFlop* mRNA. (B) Injection of 100 pg of *XFlop* mRNA at the two-cell stage (lower embryos) caused an increased thickness of the blastocoel roof when compared with control embryos (upper) at stage 9. Embryos were fixed in FG fix and split open for photography along the animal/vegetal axis. (C) The internal (blastocoelic) surfaces of animal caps from stage 9 embryos injected at the two-cell stage with 10-250 pg *XFlop* mRNA and cultured for ten minutes before fixation and staining with Alexa-488 Phalloidin. XFlop increases cortical actin assembly in a dose-dependent manner (arrow indicates a dividing cell); shown are images of whole caps (upper row) and their pixel intensity measurements (lower row). (D) Quantitative analysis of pixel intensities measured from the experiment shown in C. Five to six caps for each treatment were measured for pixel intensity quantitation. Student's *t*-test shows that XFlop increases the overall amount of cortical actin significantly in a dose-dependent manner ($P<0.01$ at all doses). (E) The wound-healing rate of bases was significantly changed by either overexpressing ($P<0.01$, yellow) or underexpressing ($P<0.001$, red) XFlop. The width of the wound from each base was measured 1 hour after animal cap removal. The ratio of the width of the wound to the diameter of the whole embryo represents the wound healing rate (*y* axis, mean±s.d.). Forty-four bases from control, 14 from Xflop-overexpressing and 33 from Xflop-depleted embryos were scored.

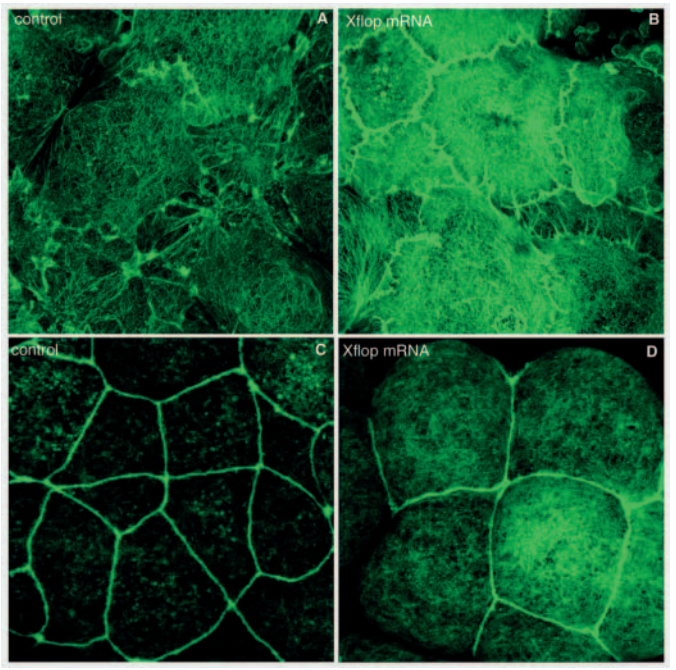

Fig. 4. High magnification confocal images showing that overexpression of XFlop increases the overall amount of cortical actin. (A,B) The cortical actin network stained with Alex-488 conjugated Phalloidin from the inner surface of control (A) and XFlop-overexpressing (B) caps. (C,D) The cortical actin network stained with Alex-488 conjugated Phalloidin from the outer surface of control (C) and XFlop-overexpressing (D) caps.

cases, there was no upregulation of cortical actin (data not shown), showing that these are specific properties of XFlop and LPA signaling.

XFlop is required for actin assembly in the early *Xenopus* embryos

We then asked whether XFlop is necessary, as well as sufficient, for actin assembly in early *Xenopus* embryos. Twelve antisense deoxyoligonucleotides were tested for their ability to deplete maternal *XFlop* mRNA. Two of these (oligo 1s and 5s) reduced the maternal store of *XFlop* mRNA to 10%, or less, of the levels in control oocytes, when doses of 8-12 ng per ooctye were used (Fig. 5A). These oligos were synthesized with the three 5′ and three 3′ phosphorodiester bonds replaced by phosphorothioate linkages. These chimeric oligos were injected, either individually or together, into cultured oocytes, which were then fertilized using the host transfer method (Holwill, 1987). *XFlop* mRNA levels remained at low levels until the gastrula stage, after which zygotic *XFlop* mRNA began to be synthesized (Fig. 5A). Therefore, the embryos can develop at least until the mid-gastrula stage with a significant depletion of *XFlop* mRNA.

At the blastula stage, XFlop-depleted embryos looked morphologically normal, but when the vitelline membranes were removed, they became less spherical than control embryos (Fig. 5B,C), which made them look a little larger when viewed from above (Fig. 5B, compare the lengths of the lines of control and depleted embryos). When fixed and bisected along the animal/vegetal axis, and viewed from the side, the less spherical architecture becomes more obvious (Fig. 5C). After excision of the animal caps, the bases healed more slowly than control bases did. After 45 minutes, the wound margins of the control bases were smooth, and the wound diameter had contracted. By contrast, the wound margins of XFlop-depleted embryos were still open (Fig. 5D). These data are quantitated and compared with the effect of XFlop overexpression in Fig. 3E. Animal caps from these embryos were cultured for 10 minutes, fixed, stained with Alexa 488-coupled phalloidin, and their blastocoelic surfaces examined by confocal microscopy. Fig. 5E shows low magnification images of whole caps (upper panels), and high magnification images (lower panels) of control and XFlop-depleted animal caps. The overall level of cortical actin staining was significantly reduced by XFlop depletion. Quantitation was performed by comparing the mean pixel intensity (±s.d.) of six caps from each treatment (Fig. 5F). In addition, none of the XFlop-depleted caps had actin-rich purse strings around their circumferences (arrow in Fig. 5E). High magnification images (Fig. 5E) show the reverse of XFlop overexpression; staining of all actin-containing structures (except for the contractile rings of dividing cells) was reduced. There were fewer cell processes, and those that were present had less actin staining than did those of controls. The cortical actin network was also reduced. As is the case for overexpression, this suggests that XFlop signaling is required to maintain the normal amount of F-actin in all actin-containing structures, except those required for cell division.

We next examined the cortical actin network in dissociated cells from control and XFlop-depleted embryos (Fig. 5G). Animal caps were dissociated and cultured in calcium/magnesium-free saline for 10 minutes before fixation and staining. This culture time is not sufficient for the cortical network to transform from the dense to the coarse network type, a process that takes at least 30 minutes (Lloyd et al., 2005). Actin staining was significantly reduced in individual dissociated cells that were XFlop depleted. This was quantitated by the comparison of mean pixel intensity (±s.d.) from 20 control and 28 XFlop-depleted cells, which showed that the decrease is statistically significant ($P<0.01$, Fig. 5H). Fig. 5G (middle panels) shows the images in rainbow scale, in which the Zeiss LSM510 software assigns different spectral colors to different pixel intensities. This illustrates the fact that, even though staining levels are reduced in XFlop-depleted embryos, there is still an actin network present, but it contains less actin. In some areas (see arrow, Fig. 5G), areas denuded of actin filaments can be seen, through which underlying yolk platelets can be seen.

In order to check whether microtubule and intermediate filament assemblies were also affected by XFlop depletion, we stained animal caps from XFlop-depleted and control late blastulae with antibodies against tubulin or cytokeratin. In the absence of maternal XFlop, the microtubule and cytokeratin networks in the animal caps were both intact, although the F-actin network was significantly reduced (Fig. 6A,B), suggesting that the cytoarchitectural defects seen at the blastula stage are primarily due to the loss of the cortical actin skeleton.

In order to show that these defects are specific for the loss of the maternal store of *XFlop* mRNA, and were not caused by non-specific degradation of other mRNAs by the oligo, or by random toxicity, we injected *XFlop* mRNA-depleted embryos at the two-cell stage with 50 pg of full-length *XFlop* mRNA.

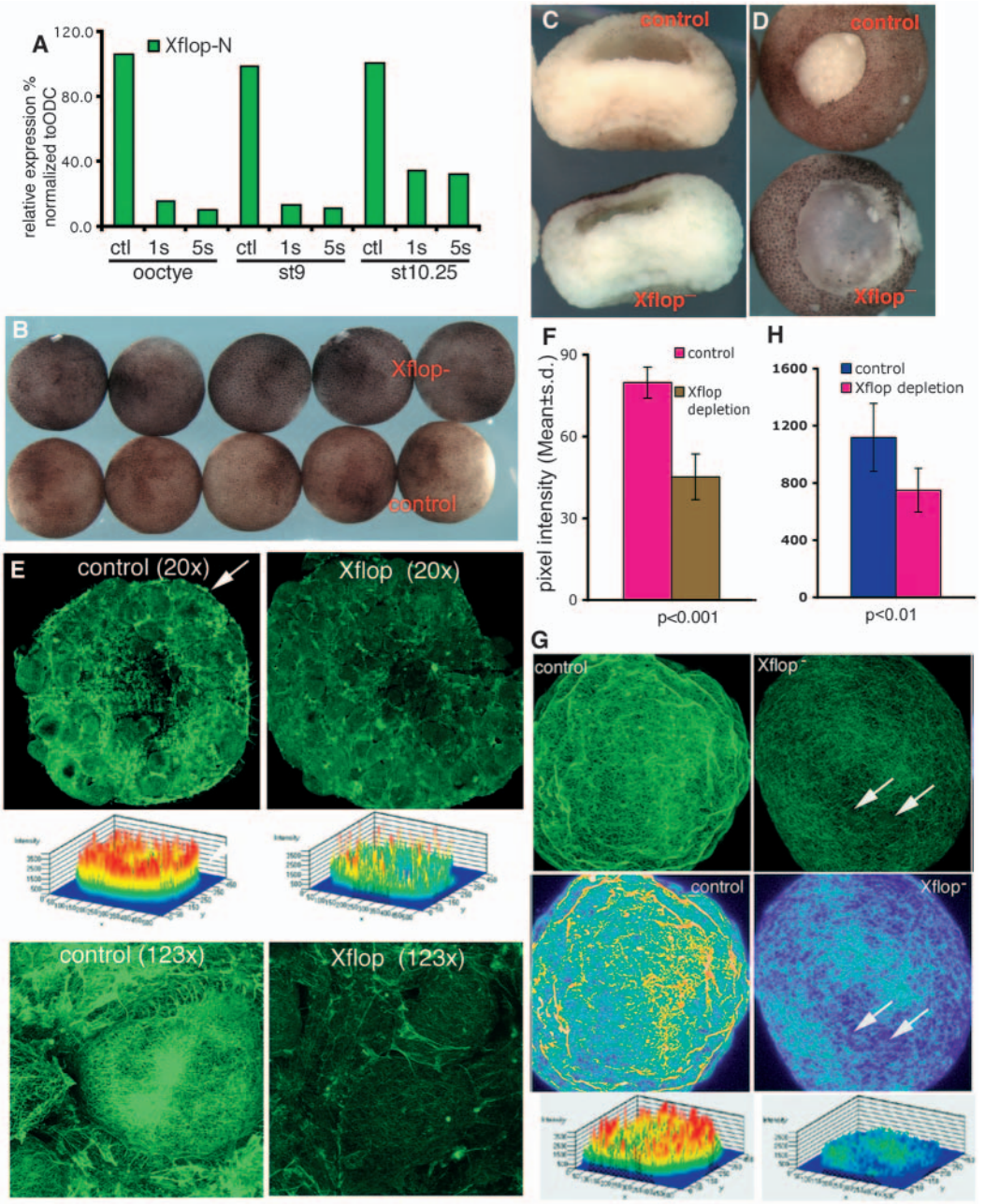

Fig. 5. XFlop is necessary for cortical actin assembly. Two antisense oligos (1s and 5s) were used to deplete the maternal store of *XFlop* mRNA in oocytes, which were then fertilized to assess the effect of maternal XFlop depletion. (A) The efficiency of depletion of *XFlop* mRNA by oligos 1s (10 ng/oocyte) and 5s (8 ng/oocyte); *XFlop* mRNA is not resynthesized before the gastrula stage. Oocyte, st.9 and st.10.25 represent the levels of *XFlop* mRNA, normalized to the level of ODC mRNA at the oocyte, late blastula and early gastrula stages. 1s and 5s represent the levels at the same stages after injection of oligo 1s and 5s, respectively. XFlop-depleted embryos were flattened when compared with control embryos, as shown from above (B), and from the side of bisected embryos (C). (D) XFlop depletion resulted in slower wound healing. Quantitation of this effect is shown, and is compared with that caused by the overexpression of XFlop in the same experiment, shown in Fig. 3E. (E) The effect of XFlop depletion on cortical actin at stage 9. XFlop depletion reduced the overall amount of cortical actin (upper panel, low-magnification confocal images; middle panel, pixel intensity; lower panel, high-magnification confocal images). (F) The decrease of the overall amount of the cortical actin caused by XFlop depletion is significant (P<0.001, n=5 independent experiments). (G) The effects of XFlop depletion on F-actin in single dissociated cells further indicate that XFlop is required for the cortical actin assembly. Twenty control and 28 XFlop-depleted cells were imaged and the pixel intensity was measured. (H) Quantitative analysis shows the decrease of the pixel intensity is significant (P<0.01).

The injected mRNA rescued the rigidity and spherical architecture of the late blastula (Fig. 6C), as well as their ability to heal wounds (Fig. 6C) and the density of the cortical actin skeleton (Fig. 6D,E). This rescue was seen in four repeat experiments. As an additional control for oligo specificity, we found that two antisense oligos targeting different regions of *XFlop* mRNA gave identical phenotypes, and that a 1:1 mixture of these two oligos had additive effects (data not shown). The XFlop-depletion phenotypes have been reproduced in five independent experiments. In wound healing assays, we analyzed five to six embryos from each treatment at late blastula stage. Taken together, these data show that XFlop is necessary, as well as sufficient, for maintenance of the correct levels of cortical actin and the maintenance of the spherical architecture of the embryo.

When embryos depleted of the maternal stockpile of *XFlop* mRNA were allowed to develop further, they exhibited defects in gastrulation movements, and post-gastrulation abnormalities (Fig. 7A-C). Defects ranged from mild (distorted axes, truncations and reduced head structures, Fig. 7B, n=10 in a single experiment) to severe (absence of head, unclosed blastopore, severe truncations, Fig. 7C, n=9 in the same experiment). We previously showed that reduction of the cortical actin skeleton by depletion of mRNA for plakoglobin

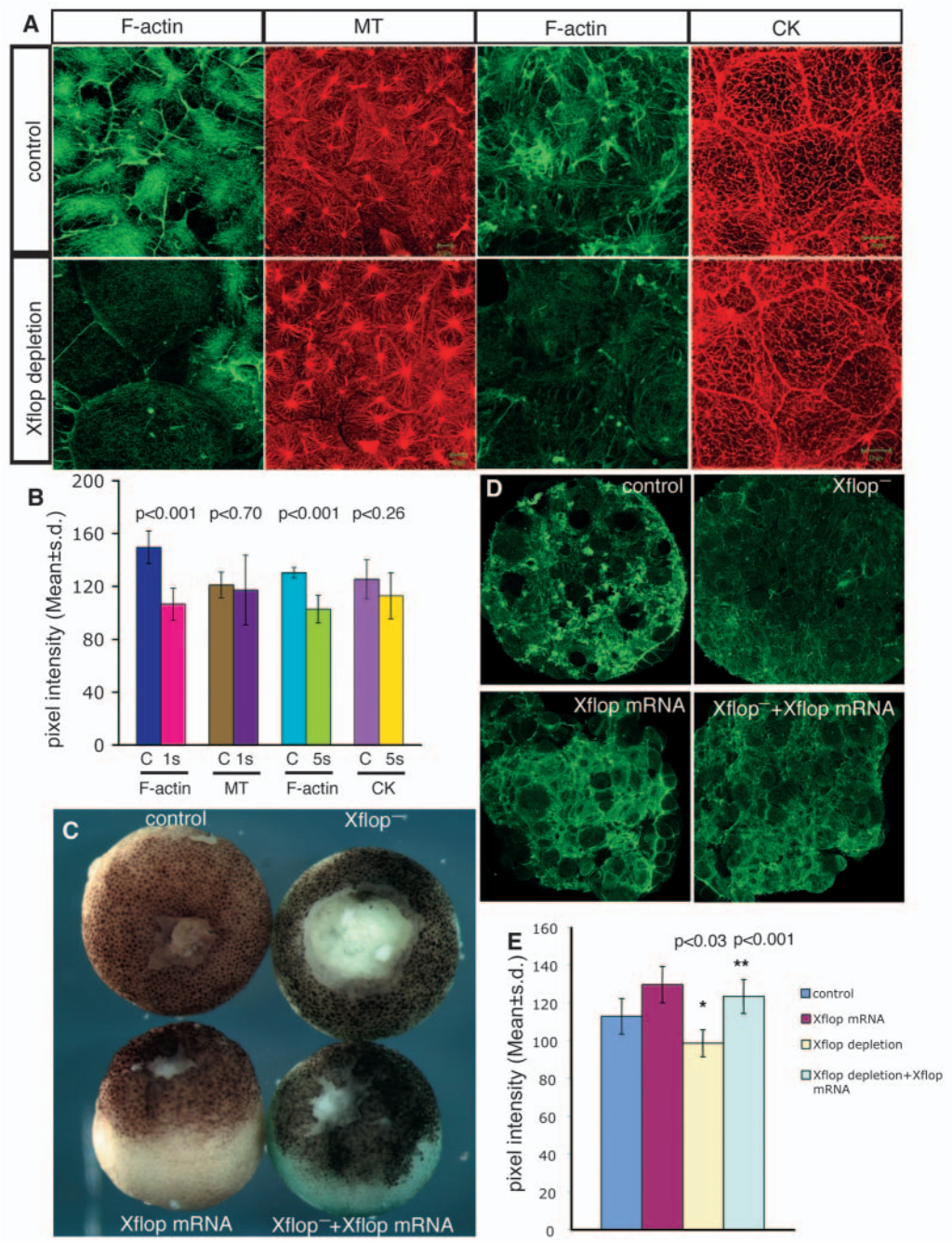

Fig. 6. XFlop depletion specifically affects the actin skeleton. (A) The microtubule and intermediate filament networks are not significantly affected by XFlop depletion. In a single experiment, control (upper row) and XFlop-depleted (lower row; oligo 1s, 12 ng; oligo 5s, 10 ng) late blastulae were divided into two groups (with five to six embryos in each). The first group was assayed for F-actin by phalloidin staining. The second group was fixed with FG fix with or without 0.5 μM Taxol for microtubule (MT) staining or cytokeratin (CK) staining, respectively. Although significant depletion of the F-actin network was seen, no significant defects in microtubule or cytokeratin filament staining was seen. (B) The decrease of F-actin observed in the experiment shown in A is significant (P<0.001; five to six caps were scored in each case). (C) The bases of control and XFlop-depleted embryos with or without injection of 100 pg *XFlop* mRNA into the animal cytoplasm at the two-cell stage. *XFlop* mRNA rescues the wound healing and loss of rigidity caused by the depletion of *XFlop* mRNA in the oocyte. (D) Cortical actin is also rescued, as shown in animal caps from the same embryos stained with Alexa-488 phalloidin. (E) Quantitative analysis of the overall amount of the cortical actin from the experiment shown in C and D (compare the control with the XFlop-depleted animal caps, P<0.03; XFlop depletion with XFlop mRNA rescue, P<0.001). The rescue experiments have been repeated four times with the similar results. In each experiment, five to six caps from each treatment were analyzed.

(Kofron et al., 2002), or the two LPA receptors LPA1 and LPA2 (Lloyd et al., 2005), causes defective gastrulation movements. This suggests that XFlop-regulated cortical actin assembly is required for normal gastrulation movements. To test this further, we microinjected *XFlop* mRNA into single animal cells at the eight-cell stage together with mRNA encoding β-galactosidase. The early ectoderm cells overexpressing XFlop do not undergo epiboly (Fig. 7D,E), the spreading movement by which cells in the animal region, destined to form the ectoderm, spread around the whole surface of the embryo during gastrulation. Thus, both depletion and overexpression of XFlop abrogate the cell movements of gastrulation. The etiology of the post-gastrulation defects is likely to be complex, first because reduced or delayed gastrulation movements will lead to later defects in a pleiotropic fashion, and second, because XFlop may be required for other aspects of early development. To address this latter point, we investigated whether XFlop is required for the cell fate specification events that take place during the blastula stage, by assaying cDNA from XFlop-depleted embryos for molecular markers of the three primary germ layers, and of the dorsal axis. All of these structures are initiated during the mid- to late-blastula stages by intercellular signaling events (Harland and Gerhart, 1997; Kofron et al., 1999; Kofron, 2003), and by localized maternal transcription factors (Kofron et al., 1999; Sundaram et al., 2003; Xanthos et al., 2002; Xanthos et al., 2001; Zhang et al.,

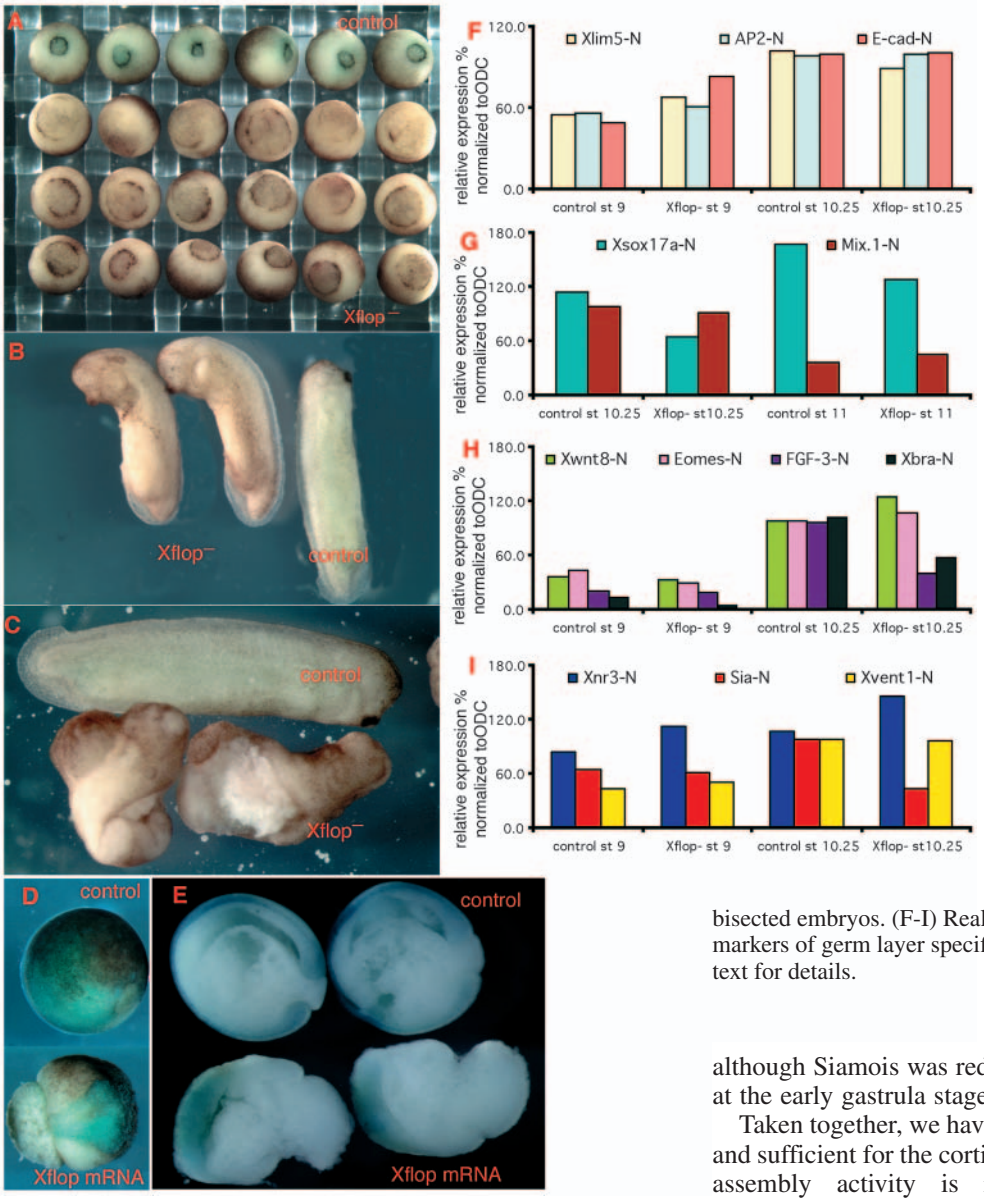

Fig. 7. XFlop is required for normal gastrulation movements and the formation of axial structures. (A) Control (blue) and XFlop-depleted (oligo 5s, 10 ng/oocyte, brown) embryos, shown when the controls were at the mid-gastrula stage (stage 11). Note, XFlop depletion caused delayed blastopore closure. (B,C) Later defects caused by depletion of the maternal *XFlop* mRNA, ranging from open neural folds and poorly formed axial structures in 50% of cases (B, *n*=10), to distorted body axes in the other 50% (C, *n*=9). (D,E) Overexpression of XFlop interferes with epiboly and gastrulation movements. (D) Embryos at the end of gastrulation that were injected with either 500 pg β-galactosidase mRNA only (upper embryo), or with 500 pg β-galactosidase mRNA and 100 pg *XFlop* mRNA, into a single animal cytoplasm at the eight-cell stage. In control embryos, the blue β-galactosidase stain has spread around the embryo surface as epiboly of the animal cap cells takes place. In *XFlop* mRNA-injected embryos, the clone from the injected animal cell has failed to undergo epiboly. (E) The same experiment that is shown in D shown in bleached and mid-sagitally bisected embryos. (F-I) Real-time RT-PCR analysis for early zygotic markers of germ layer specification and dorsal axis formation. See text for details.

1998). Early zygotic markers of ectoderm (Xlim5, AP2 and E-cadherin) (Houston and Wylie, 2003; Luo et al., 2002), mesoderm (Eomesodermin, Fgf8, Xbra and Xwnt8), endoderm (Xsox17 and Mix.1) (Xanthos et al., 2002), and of the dorsoventral axis (Xnr3, Siamois and Xvent1) (Yokota et al., 2003) were analyzed at late blastula (stage 9) and early gastrula (stage 10.25) stages, using quantitative real-time RT-PCR techniques. Expression of neither the early ectodermal nor the early endodermal genes were changed dramatically (Fig. 7F,G), indicating that XFlop is not necessary for the specification of ectoderm and endoderm. The expression of Fgf3 and Xbra were reduced, but not absent, at the beginning of gastrulation (Fig. 7H). Because Xwnt8 and Eomesdermin were activated on time, this suggests that XFlop may be necessary for the full activation of a subgroup of mesodermal genes. This is also consistent with the gastrulation movement failure, as shown in Fig. 7A-C. The depletion of XFlop does not affect the activation of early dorsal markers (Fig. 7I), although Siamois was reduced, when compared with controls, at the early gastrula stage.

Taken together, we have shown that XFlop is both necessary and sufficient for the cortical actin assembly, and that this actin assembly activity is required for normal gastrulation movements.

XFlop and LPA signaling play distinct roles in cortical actin assembly

We have recently shown that a different signaling pathway, mediated by the phospholipid ligand lysophosphatidic acid (LPA), and its two receptors XLPA1 and XLPA2, also controls the cortical actin skeleton of the early *Xenopus* embryo, so it was important to establish the relationship between these two signaling pathways. In particular, we wanted to test whether each pathway independently initiates actin assembly, or whether they are in the same pathway.

A comparison of XFlop overexpression and depletion (Figs 3-6) with previously published data on LPA1 and LPA2 depletion (Lloyd et al., 2005) suggests that the two signaling pathways control different aspects of actin assembly. LPA depletion causes the dense actin network characteristic of interphase blastomeres in vivo to become replaced by the coarser network seen in dividing blastomeres in vivo, or in dissociated blastomeres (Lloyd et al., 2005). Overexpression of

XFlop, however, caused a general increase in actin in all actin-containing structures (Figs 3, 4), whereas its depletion caused an overall decrease in the actin present in all actin-containing structures (Figs 5, 6) without causing a shift to the looser network characteristic of dividing or dissociated cells. This would suggest that LPA1/2 and XFlop play different roles in actin assembly.

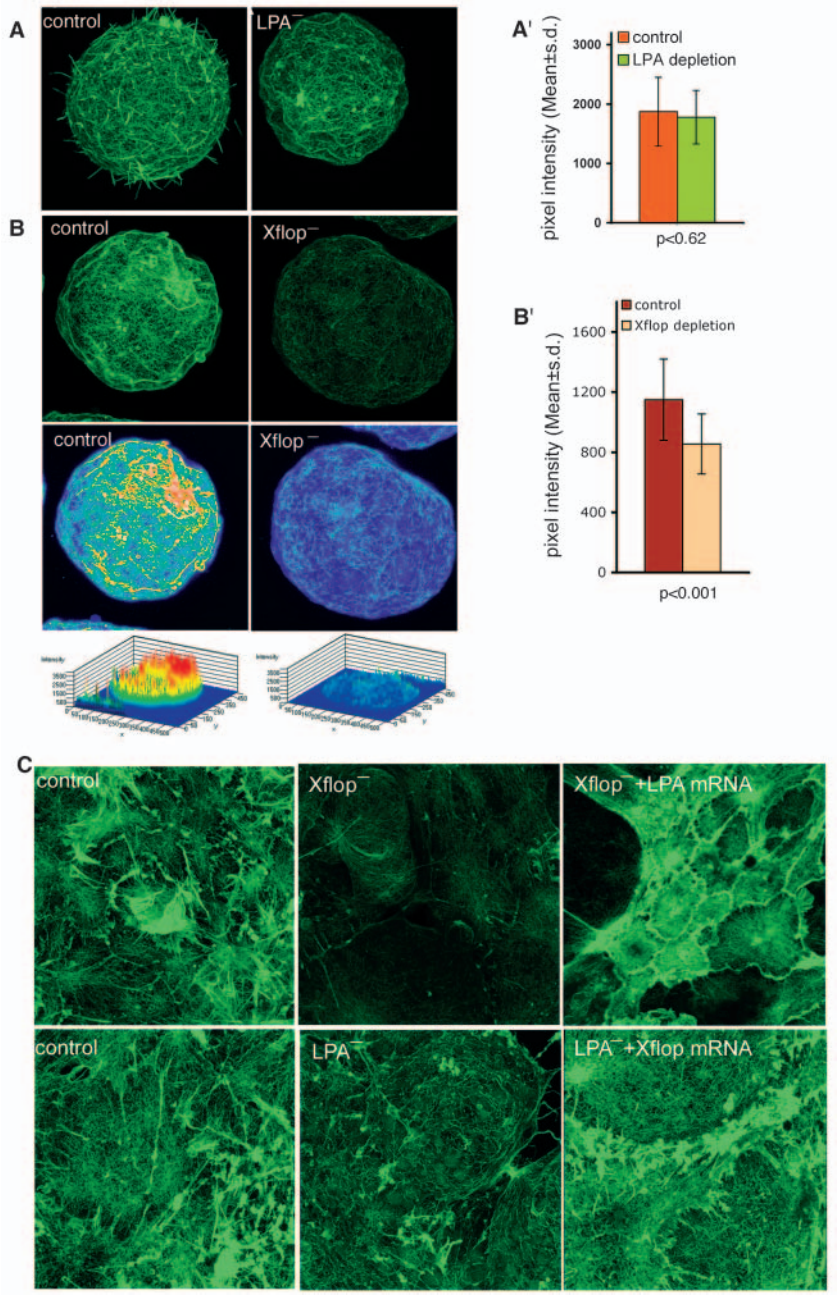

Fig. 8. XFlop and LPA have distinct roles in cortical actin assembly. (A,A′) Single dissociated cells from control, and LPA1 and LPA2 receptor-depleted embryos (15 ng of the morpholino oligo was used against each receptor). Depletion of the LPA receptors reduced the density of cortical actin to that of control dissociated cells (see also Lloyd et al., 2005). (B,B′) Single dissociated cells from control and XFlop-depleted (12 ng/oocyte, oligo 1s) embryos. XFlop depletion reduces cortical actin significantly when compared with control dissociated cells. (C) *XFlop* and LPA mRNA can each rescue the effects of depletion of the other, indicating that they have distinct functions in actin assembly. For experimental details, see text.

To confirm this, we further investigated the effects of XFlop and LPA1 and LPA2 depletions in dissociated cells from late blastulae. Animal caps were excised at stage 9, dissociated in Ca^{2+}/Mg^{2+}-free 1×MMR, and cultured for 90 minutes. Under these conditions, dissociated blastomeres adopt the coarse configuration of cortical actin that is characteristic of dividing cells in intact animal caps (Lloyd et al., 2005). Phalloidin-stained, single dissociated blastomeres from embryos depleted of LPA1 and LPA2 (Fig. 8A) or Xflop (Fig. 8B) are shown. Quantitation of total cortical actin by pixel intensity measurements of 10 control and 27 LPA1 and LPA2-depleted blastomeres, showed that LPA1 and LPA2 depletion did not significantly reduce the amount of cortical actin in each isolated blastomere (Fig. 8A′) (see also Lloyd et al., 2005). Xflop depletion, however, did significantly reduce the total amount of cortical actin in isolated blastomeres (Fig. 8B,B′). This reduction was quantitated by comparing the mean pixel intensity of 30 individual control and 44 XFlop-depleted blastomeres (Fig. 8B′), and suggests that XFlop controls the overall level of actin assembly.

To test further whether XFlop and LPA lie in the same pathway, we investigated whether depletion of one would block the effect of overexpression of the other. If they lie in the same pathway, then they will be epistatic; one will rescue the other, but the reverse will not be the case. Oocytes depleted of either LPA1 and LPA2, or XFlop, were fertilized, and mRNA encoding either XFlop or LPA1 was injected into the animal cytoplasm at the two-cell stage. Both LPA1 overexpression in XFlop-depleted embryos, and XFlop overexpression in LPA1 and LPA2-depleted embryos, increased the levels of cortical actin (Fig. 8C). This shows that neither receptor requires the other for its action, and strongly suggests that they have separate roles in cortical actin assembly.

Discussion

A cortical network of F-actin has been described at the earliest stages of embryogenesis of a number of species, including *Drosophila* (Karr and Alberts, 1986; Warn and Robert-Nicoud, 1990), mouse (Albertini et al., 1987), pig (Reima et al., 1993) and *C. elegans* (Strome, 1986). However, little is known about the mechanisms by which each cell of the early embryo synthesizes a specific pattern and density of cortical actin. Forward genetic screens in *Drosophila* have revealed a number of genes involved in actin dynamics (Postner et al., 1992; Postner and Wieschaus, 1994; Schejter and Wieschaus, 1993; Straub et al., 1996; Sullivan et al., 2000), but most of these studies focused specifically upon cellularization, the process by which a syncytial blastula changes to

a cellular blastula. None of the genes identified so far in these studies suggest a role for intercellular signaling. Here, we show that expression screening is a useful tool for identifying proteins involved in cytoskeletal assembly in early embryos. It allows rapid gain-of-function experiments by the injection of mRNA pools or single mRNAs, and rapid confirmation of function by loss-of-function experiments. Most proteins functioning at the blastula stages in *Xenopus* are encoded by genes expressed in the oocyte, and whose mRNA is stored in the egg. Depletion of this mRNA by antisense oligonucleotide injection into cultured oocytes, followed by fertilization of the oocytes, allows any essential role of the cognate protein to be rapidly identified. In this study, and elsewhere (Lloyd et al., 2005), we have used these assays to show that in a cellular vertebrate embryo, intercellular signaling plays a primary role in the control of F-actin assembly in each cell. Here, we show that the G protein-coupled receptor XFlop is both necessary and sufficient for this process. It is interesting that two G protein-coupled receptors (the LPA receptors are also GPCRs) have now been identified that seem to perform separate, but overlapping roles in the assembly of the correct pattern and density of actin filaments in the embryonic cell cortex.

XFlop is most closely related to mammalian GPR4, a member of a recently proposed sub-family of G protein-coupled receptors, the OGR1 sub-family (Xu, 2002). Comprising OGR1 (ovarian cancer G protein-coupled receptor 1), G2A (G2 accumulation), TDAG8 (T cell death-associated gene 8) and GPR4 (G protein-coupled receptor 4), the sub-family is moderately conserved, with 36-51% amino acid identity. Ligands for this group are still being identified, but include related signaling lipids. TDAG8 has been reported to bind psychosine (galactosyl sphingosine) (Im et al., 2001), whilst OGR1 binds sphingosylphosphoryl choline (SPC) (Xu et al., 2000), and GPR4 and 2GA bind both SPC and lyso-phosphatidyl choline (LPC) (Bektas et al., 2003; Kabarowski et al., 2001; Zhu et al., 2001). More recently, it has been reported that OGR1 and GPR4 respond differentially to changes in extracellular proton concentration (Ludwig et al., 2003). OGR1 increases inositol phosphate formation, whilst GPR4 increases cyclic AMP formation, in response to increased proton concentration. Ligand specificities have generally been identified by overexpressing the receptor in cultured cells, so it is not yet clear which ligands are used in vivo, and whether these change spatially and temporally during tissue differentiation, nor are the in vivo functions of the OGR1 sub-family fully established. G2A null mice have an abnormal expansion of both B and T lymphocytes, and an autoimmune syndrome, suggesting that G2A acts as a repressor in the immune system (Le et al., 2001). GPR4 is thought to mediate the growth stimulatory effects of SPC on Swiss 3T3 cells, whilst OGR1 may mediate the inhibitory growth effects of this same ligand (Xu et al., 2000; Zhu et al., 2001), suggesting complementary functions of these related receptors. We show here that a related receptor, XFlop, in *Xenopus*, plays an essential in vivo role in the assembly of the correct amount of cortical actin. It will be interesting to study the related mammalian receptors in this respect, to see whether this function is conserved throughout the vertebrates.

Signaling through G protein-coupled receptors has been implicated previously in the control of actin assembly, particularly in cell responses to chemotactic stimuli. Ligands for these can be small molecules such as cAMP (reviewed by Hereld and Devreotes, 1992), peptide ligands such as stromal derived factor 1 (SDF1) (Nagasawa et al., 1999), or N-formyl methionine peptides (Panaro and Mitolo, 1999). However, the role of intercellular signaling in establishing the amount, and pattern, of cortical actin that maintains the correct shape and rigidity of the early embryo is less well understood. During the egg to blastula stages, the number of cells in the embryo doubles with each cell cycle. However, after each division cycle, each cell assembles the cortical actin network appropriate to the shape and rigidity of the whole embryo. In general, this could be accomplished by intracellular components of the actin polymerization machinery inherited from the egg, or by intercellular signaling. This work, and a previous paper (Lloyd et al., 2005), shows that at least two intercellular signaling pathways control this process in early *Xenopus* embryos. The role of the XFlop-mediated pathway appears to be to control the overall amount of F-actin in most, but not all, actin-containing structures, as XFlop depletion causes reduced F-actin in all structures except the contractile rings of cytokinesis, which must be controlled by other signals. By contrast, the role of LPA signaling seems to be to control the switch from dense cortical actin during interphase to a less dense network during cytokinesis (Lloyd et al., 2005). The two pathways can also be distinguished by the fact that each can be initiated in the absence of the other.

The ligand for XFlop has yet to be identified, as have details of its downstream signaling pathways. The multiple effects of XFlop depletion (reduction in the cortical network and cell processes, and absence of wound healing and purse-string formation), and the fact that overexpression increases the amount of F-actin without amplifying only one type of actin-containing structure, suggest that it acts through more than one downstream signaling pathway. It will be important to identify which cytoplasmic signaling intermediates, and which of their effectors, act downstream of LPA and XFlop signaling at the cell surface in this in vivo developing system.

The authors would like to thank the NIH for financial support (RO1 HD044764, T32HD07463), and Bertie Puck for excellent technical support.

References

Albertini, D. F., Overstrom, E. W. and Ebert, K. M. (1987). Changes in the organization of the actin cytoskeleton during preimplantation development of the pig embryo. *Biol. Reprod.* **37**, 441-451.

Bause, E. (1983). Structural requirements of N-glycosylation of proteins. Studies with proline peptides as conformational probes. *Biochem. J.* **209**, 331-336.

Bektas, M., Barak, L. S., Jolly, P. S., Liu, H., Lynch, K. R., Lacana, E., Suhr, K. B., Milstien, S. and Spiegel, S. (2003). The G protein-coupled receptor GPR4 suppresses ERK activation in a ligand-independent manner. *Biochemistry* **42**, 12181-12191.

Chung, H. A., Hyodo-Miura, J., Kitayama, A., Terasaka, C., Nagamune, T. and Ueno, N. (2004). Screening of FGF target genes in Xenopus by microarray: temporal dissection of the signalling pathway using a chemical inhibitor. *Genes Cells* **9**, 749-761.

Grammer, T. C., Liu, K. J., Mariani, F. V. and Harland, R. M. (2000). Use of large-scale expression cloning screens in the Xenopus laevis tadpole to identify gene function. *Dev. Biol.* **228**, 197-210.

Harland, R. and Gerhart, J. (1997). Formation and function of Spemann's organizer. *Annu Rev Cell Dev. Biol.* **13**, 611-667.

Heiber, M., Docherty, J. M., Shah, G., Nguyen, T., Cheng, R., Heng, H. H., Marchese, A., Tsui, L. C., Shi, X., George, S. R. et al. (1995). Isolation

of three novel human genes encoding G protein-coupled receptors. *DNA Cell Biol.* **14**, 25-35.

Hereld, D. and Devreotes, P. N. (1992). The cAMP receptor family of Dictyostelium. *Int. Rev. Cytol.* **137B**, 35-47.

Holwill, S., Heasman, J., Crawley, C. and Wylie, C. C. (1987). Axis and germ line deficiencies caused by u.v irradiation of Xenopus oocytes cultured in vitro. *Development* **100**, 735-743.

Houston, D. W. and Wylie, C. (2003). The Xenopus LIM-homeodomain protein Xlim5 regulates the differential adhesion properties of early ectoderm cells. *Development* **130**, 2695-2704.

Im, D. S., Heise, C. E., Nguyen, T., O'Dowd, B. F. and Lynch, K. R. (2001). Identification of a molecular target of psychosine and its role in globoid cell formation. *J. Cell Biol.* **153**, 429-434.

Kabarowski, J. H., Zhu, K., Le, L. Q., Witte, O. N. and Xu, Y. (2001). Lysophosphatidylcholine as a ligand for the immunoregulatory receptor G2A. *Science* **293**, 702-705.

Karr, T. L. and Alberts, B. M. (1986). Organization of the cytoskeleton in early Drosophila embryos. *J. Cell Biol.* **102**, 1494-1509.

Kofron, M., Demel, T., Xanthos, J., Lohr, J., Sun, B., Sive, H., Osada, S., Wright, C., Wylie, C. and Heasman, J. (1999). Mesoderm induction in Xenopus is a zygotic event regulated by maternal VegT via TGFbeta growth factors. *Development* **126**, 5759-5770.

Kofron, M., Heasman, J., Lang, S. A. and Wylie, C. C. (2002). Plakoglobin is required for maintenance of the cortical actin skeleton in early Xenopus embryos and for cdc42-mediated wound healing. *J. Cell Biol.* **158**, 695-708.

Kofron, M., Xanthos, J. and Heasman, J. (2003). Maternal VegT and beta-catenin: patterning the Xenopus blastula. In *The Vertebrate Organizer* (ed. H. Grunz), pp. 1-9. Essen, Germany: Springer.

Le, L. Q., Kabarowski, J. H., Weng, Z., Satterthwaite, A. B., Harvill, E. T., Jensen, E. R., Miller, J. F. and Witte, O. N. (2001). Mice lacking the orphan G protein-coupled receptor G2A develop a late-onset autoimmune syndrome. *Immunity* **14**, 561-571.

Lloyd, B., Tao, Q., Lang, S. and Wylie, C. (2005). Lysophosphatidic acid signaling controls cortical actin assembly and cytoarchitecture in Xenopus embryos. *Development* **132**, 805-816.

Ludwig, M. G., Vanek, M., Guerini, D., Gasser, J. A., Jones, C. E., Junker, U., Hofstetter, H., Wolf, R. M. and Seuwen, K. (2003). Proton-sensing G-protein-coupled receptors. *Nature* **425**, 93-98.

Luo, T., Matsuo-Takasaki, M., Thomas, M. L., Weeks, D. L. and Sargent, T. D. (2002). Transcription factor AP-2 is an essential and direct regulator of epidermal development in Xenopus. *Dev. Biol.* **245**, 136-144.

Nagasawa, T., Tachibana, K. and Kawabata, K. (1999). A CXC chemokine SDF-1/PBSF: a ligand for a HIV coreceptor, CXCR4. *Adv. Immunol.* **71**, 211-228.

Nieuwkoop, P. D. A. F. J. (1975). Normal table of Xenopus laevis (Daudin). Amersterdam: North-Holland.

Oliveira, L., Paiva, A. C., Sander, C. and Vriend, G. (1994). A common step for signal transduction in G protein-coupled receptors. *Trends Pharmacol. Sci.* **15**, 170-172.

Panaro, M. A. and Mitolo, V. (1999). Cellular responses to FMLP challenging: a mini-review. *Immunopharmacol. Immunotoxicol.* **21**, 397-419.

Postner, M. A. and Wieschaus, E. F. (1994). The nullo protein is a component of the actin-myosin network that mediates cellularization in Drosophila melanogaster embryos. *J. Cell Sci.* **107**, 1863-1873.

Postner, M. A., Miller, K. G. and Wieschaus, E. F. (1992). Maternal effect mutations of the sponge locus affect actin cytoskeletal rearrangements in Drosophila melanogaster embryos. *J. Cell Biol.* **119**, 1205-1218.

Quaas, J. and Wylie, C. (2002). Surface contraction waves (SCWs) in the Xenopus egg are required for the localization of the germ plasm and are dependent upon maternal stores of the kinesin-like protein Xklp1. *Dev. Biol.* **243**, 272-280.

Reima, I., Lehtonen, E., Virtanen, I. and Flechon, J. E. (1993). The cytoskeleton and associated proteins during cleavage, compaction and blastocyst differentiation in the pig. *Differentiation* **54**, 35-45.

Revenu, C., Athman, R., Robine, S. and Louvard, D. (2004). The co-workers of actin filaments: from cell structures to signals. *Nat. Rev. Mol. Cell Biol.* **5**, 635-646.

Robb, D. L., Heasman, J., Raats, J. and Wylie, C. (1996). A kinesin-like protein is required for germ plasm aggregation in Xenopus. *Cell* **87**, 823-831.

Schejter, E. D. and Wieschaus, E. (1993). Functional elements of the cytoskeleton in the early Drosophila embryo. *Annu. Rev. Cell Biol.* **9**, 67-99.

Straub, K. L., Stella, M. C. and Leptin, M. (1996). The gelsolin-related flightless I protein is required for actin distribution during cellularisation in Drosophila. *J. Cell Sci.* **109**, 263-270.

Strome, S. (1986). Fluorescence visualization of the distribution of microfilaments in gonads and early embryos of the nematode Caenorhabditis elegans. *J. Cell Biol.* **103**, 2241-2252.

Sullivan, R., Burnham, M., Torok, K. and Koffer, A. (2000). Calmodulin regulates the disassembly of cortical F-actin in mast cells but is not required for secretion. *Cell Calcium* **28**, 33-46.

Sundaram, N., Tao, Q., Wylie, C. and Heasman, J. (2003). The role of maternal CREB in early embryogenesis of *Xenopus laevis*. *Dev. Biol.* **261**, 337-352.

Torpey, N., Wylie, C. C. and Heasman, J. (1992). Function of maternal cytokeratin in Xenopus development. *Nature* **357**, 413-415.

Vernos, I., Raats, J., Hirano, T., Heasman, J., Karsenti, E. and Wylie, C. (1995). Xklp1, a chromosomal Xenopus kinesin-like protein essential for spindle organization and chromosome positioning. *Cell* **81**, 117-127.

Warn, R. M. and Robert-Nicoud, M. (1990). F-actin organization during the cellularization of the Drosophila embryo as revealed with a confocal laser scanning microscope. *J. Cell Sci.* **96**, 35-42.

Wheatley, M. and Hawtin, S. R. (1999). Glycosylation of G-protein-coupled receptors for hormones central to normal reproductive functioning: its occurrence and role. *Hum. Reprod. Update* **5**, 356-364.

Xanthos, J. B., Kofron, M., Wylie, C. and Heasman, J. (2001). Maternal VegT is the initiator of a molecular network specifying endoderm in Xenopus laevis. *Development* **128**, 167-180.

Xanthos, J. B., Kofron, M., Tao, Q., Schaible, K., Wylie, C. and Heasman, J. (2002). The roles of three signaling pathways in the formation and function of the Spemann Organizer. *Development* **129**, 4027-4043.

Xu, Y. (2002). Sphingosylphosphorylcholine and lysophosphatidylcholine: G protein-coupled receptors and receptor-mediated signal transduction. *Biochim. Biophys. Acta* **1582**, 81-88.

Xu, Y., Zhu, K., Hong, G., Wu, W., Baudhuin, L. M., Xiao, Y. and Damron, D. S. (2000). Sphingosylphosphorylcholine is a ligand for ovarian cancer G-protein-coupled receptor 1. *Nat. Cell Biol.* **2**, 261-267.

Yokota, C., Kofron, M., Zuck, M., Houston, D. W., Isaacs, H., Asashima, M., Wylie, C. C. and Heasman, J. (2003). A novel role for a nodal-related protein; Xnr3 regulates convergent extension movements via the FGF receptor. *Development* **130**, 2199-2212.

Zhang, J., Houston, D. W., King, M. L., Payne, C., Wylie, C. and Heasman, J. (1998). The role of maternal VegT in establishing the primary germ layers in Xenopus embryos. *Cell* **94**, 515-524.

Zhu, K., Baudhuin, L. M., Hong, G., Williams, F. S., Cristina, K. L., Kabarowski, J. H., Witte, O. N. and Xu, Y. (2001). Sphingosylphosphorylcholine and lysophosphatidylcholine are ligands for the G protein-coupled receptor GPR4. *J. Biol. Chem.* **276**, 41325-41335.